Symbiosis

ISSN Online: 2376-4589
www.symbiosisonlinepublishing.com

Research Article | SOJ Biochemistry | Open Access

# Chemical Reactivity Properties of Standard Aromatic Amino Acids Studied by Means of Conceptual Density Functional Theory

**Norma Flores-Holguin[1], Juan Frau[2] and Daniel Glossman-Mitnik[*1, 2]**

*[1]NANOCOSMOS Virtual Lab, Department of Environment and Energy, Advanced Materials Research Center, Miguel de Cervantes 120, Complejo Industrial Chihuahua, Chihuahua Chih 31136, Mexico.*

*[2]Departament of Chemistry, University of the Balearic Islands, Palma de Mallorca 07122, Spain.*

**Received: 21 February, 2019; Accepted: 15 March, 2019; Published: 22 March, 2019**

***Corresponding author:** : Dr. Daniel Glossman-Mitnik, NANOCOSMOS Virtual Lab, Department of Environment and Energy, Advanced Materials Research Center, Miguel de Cervantes 120, Complejo Industrial Chihuahua, Chihuahua Chih 31136, Mexico, Tel: +526144391151; E-mail: daniel.glossman@cimav.edu.mx or dglossman@gmail.com*

## Abstract

This study assessed eight density functionals that include CAM-B3LYP, LC- ωPBE, M11, MN12SX, N12SX, ωB97, ωB97X and ωB97XD related to the Def2TZVP basis sets together with the SMD solvation model in the calculation of the molecular properties and structures of the four standard aromatic amino acids: Histidine, Phenylalanine, Tryptophan and Tyrosine.. The global chemical reactivity descriptors for the systems are calculated via the Conceptual Density Functional Theory (CDFT). The prediction of the maximum absorption wavelength directly from the HOMO-LUMO tends to be considerably accurate relative to the experimental values for the MN12SX density functional. Additionally, the ability of the studied molecules in acting as efficient inhibitors of the formation of Advanced Glycation Endproducts (AGEs) (perhaps as neutraceuticals), which constitutes a useful knowledge for the development of drugs for fighting Diabetes, Alzheimer and Parkinson diseases. Finally, the bioactivity scores for the four standard aromatic amino acids are predicted through different methodologies.

**Keywords:** Conceptual DFT; Chemical Reactivity Theory; Histidine; Phenylalanine; Tryptophan; Tyrosine; Aromatic Amino Acids.

## Introduction

The sea is an inexhaustible source of natural resources that give rise to molecules that can serve as a guide for the development of new medicines. For this reason, numerous investigations have been carried out in recent years dedicated to the search for new natural products that can be obtained from the knowledge of marine species [1].

Among the chemical species that can be obtained from natural products of marine origin stand out the peptides that are molecules of intermediate size between amino acids and proteins. The therapeutic application of these peptides, called for this reason therapeutic peptides, is currently one of the most active fields of research due to the great possibilities they represent as aids for the treatment of numerous diseases [2].

For the consideration of therapeutic peptides from the point of view of medicine it is necessary to know their molecular properties and their bioactivity. It is our belief that the bioactivity of these peptides is intimately related to their chemical reactivity from a molecular perspective [3, 4]. For this reason, we consider it essential to study the chemical reactivity of natural products that have the potential to become medicines through the tools provided by Computational Chemistry and Molecular Modeling. Probably the most powerful tool currently available to study the chemical reactivity of molecular systems from the point of view of Computational Chemistry and Molecular Modeling is the Conceptual DFT (CDFT), also called Chemical Reactivity Theory, which using a series of global descriptors allow to predict the interactions between molecules and understand the way in that chemical reactions proceed [5-7, 9].

The objective of this work is to study the chemical reactivity of the four standard aromatic amino acids: Histidine, Phenylalanine, Tryptophan and Tyrosine using the techniques of CDFT, determining its global properties, that is, of the molecule as a whole. Likewise, the potential ability of these amino acids to act as inhibitors of the formation of Advanced Glycation Endproducts (AGEs) will be established according to our previous ideas, and the descriptors of bioavailability and bioactivity (Bioactivity Scores) will be calculated through different procedures described in the literature [10-12].

## Theoretical Background

As this work is a part of an ongoing study related to our project on Computational Medicinal Nanochemistry, the theoretical background will be similar to that presented in previous works and will be shown here again for completeness reasons [13-20]. As in those previous works, we will be using the Kohn-Sham theory which involves the calculation of the molecular density, energy of the system, and the orbital energies particularly associated with the frontier orbitals including the Highest Occupied Molecular Orbital (HOMO) and Lowest Unoccupied Molecular Orbital (LUMO) [22-24]. This theory is necessary for establishing the quantitative values of the various

CDFT descriptors. Recently, there has been an increased interest in using range-separated (RS) exchange correlation functionals in Kohn-Sham DFT [25-28]. These functionals tend to partition the $r_{12}^{-1}$ operator and exchange the parts into long- and short-ranged parts, whose range separation parameter, $\omega$, controls the rate of attaining the long-range behavior. It is possible to fix the value of ω or "tune" it by a system-by-system mechanism that minimizes a tuning norm. The basis of the optimal tuning approach is the fact that the energy of the HOMO, $\in_H (N)$, in case of the exact Kohn-Sham (KS) theory as well as generalized KS theory for an N electron system should be -IP(N). Here, IP represents the vertical ionization potential, which is calculated as the energy difference, $E(N\text{-}1) - E(N)$, by considering a particular functional. If approximate functionals are used, it would possibly lead to considerable differences between $E_H(N)$ and $-IP(N)$. Optimal tuning involves determining the system-specific range-separation parameter, ω, non-empirically with an RSE functional. Alternatively, it also implies that several other parameters including $\in_H (N) = -IP(N)$ are optimally satisfied [29-36]. Even though there is no equivalent form to match this prescription for deriving the electron affinity (EA) together with the LUMO in case of neutral species, it is possible to say that $\in_H (N+1) = -EA(N)$, which facilitates obtaining the optimized value of ω, which is then optimized to establish both properties. This would make it easy to predict the CDFT descriptors. In the past, a simultaneous prescription referred to as the "KID procedure", owing to its correspondences with the Koopmans' theorem, was proposed by the authors [13-20]. As it has been explained in the last referenced works, KID stands for "Koopmans in DFT" and is a procedure to check the verification of the $\in_H (N) = -IP(N)$ satisfaction and at the same time a comparison between the $\in_L (N)$ of the neutral species (the LUMO) and the $\in_H (N\text{-}1)$ for the anionic system (the SOMO). The descriptor related to this comparison is called $\Delta SL$ [13-20].

## Settings and Computational Methods

This study obtained the molecular structure of the four standard aromatic amino acids: Histidine, Phenylalanine, Tryptophan and Tyrosine from Pub-Chem (https://pubchem.ncbi.nlm.nih.gov), a website that serves as the public repository for information pertaining chemical substances along with their associated biological activities. The pre-optimization of the resultant system involved selecting the most stable conformers. The selection was done using random sampling that involved molecular mechanics techniques and inclusion of the various torsional angles via the general MMFF94 force field involving the Marvin View 17.15 program, which constitutes as an advanced chemical viewer suited to multiple and single chemical queries, structures, and reactions (https://www.chemaxon.com) [37-41]. After that, the chemistry of the structures was checked and the 3D structures of the stereoisomers were generated using the same Marvin View 17.15 program. The chirality at the stereogenic centers was verified in accordance to the Cahn-Ingold-Prelog priority rules. The resulting geometries were further refined as it was explained before and the lowest energy conformation for each molecule was chosen to calculate the electronic energy and the HOMO and LUMO orbitals at the DFT functional level as mentioned in the next paragraph.

Consistent with our previous work, the computational studies were performed with the Gaussian 09 series of programs that implement density functional methods [13-20, 42]. The basis set Def2SVP was used in this work for geometry optimization and frequency determination, while the Def2TZVP basis set was used for calculating electronic properties [43, 44]. All calculations were performed in the presence of water as solvent under the Solvation Model Density (SMD) parameterization of the Integral Equation Formalism- Polarized Continuum Model (IEF-PCM) [45].

To calculate the molecular structure and properties of the studied systems, we have chosen eight density functionals which is known to consistently provide satisfactory results for several structural and thermodynamic properties: CAM-B3LYP [27], LC-ωPBE [46], M11 [47], MN12SX [48], N12SX [48], ωB97, ωB97X and ωB97XD [26].

The SMILES notations of the studied compounds were fed in the online Molinspiration software from Molinspiration Cheminformatics (www.molinspiration.com) for the calculation of the molecular properties (Log P, Total polar surface area, number of hydrogen bond donors and acceptors, molecular weight, number of atoms, number of rotatable bonds, etc.) and for the prediction of the bioactivity score for different drug targets (GPCR ligands, Kinase inhibitors, Ion channel modulators, Enzymes and Nuclear receptors). The bioactivity scores were compared with those obtained through the use of other software like MolSoft from Molsoft L.L.C. (http://molsoft.com/mprop/) and Chem Doodle Version 9.02 from iChem Labs L.L.C. (www.chemdoodle.com).

## Results and Discussion

### Molecular Structure Optimization and Verification of the KID Procedure

The molecular structures of the optimized conformers of the four standard aromatic amino acids obtained as mentioned in the Settings and Computational Methods section, and whose graphical sketches are shown in Figure 1, were reoptimized in the gas phase by considering the DFTBA model available in Gaussian 09 and then optimized again using the eight density functionals mentioned in the previous section together with the Def2SVP basis set and the SMD solvent model using water as the solvent. After verifying that each of the structures corresponded to the minimum energy conformations through a frequency calculation analysis, the electronic properties were determined by using the same model chemistry but with the Def2TZVP basis set instead of that used for the geometry optimization.

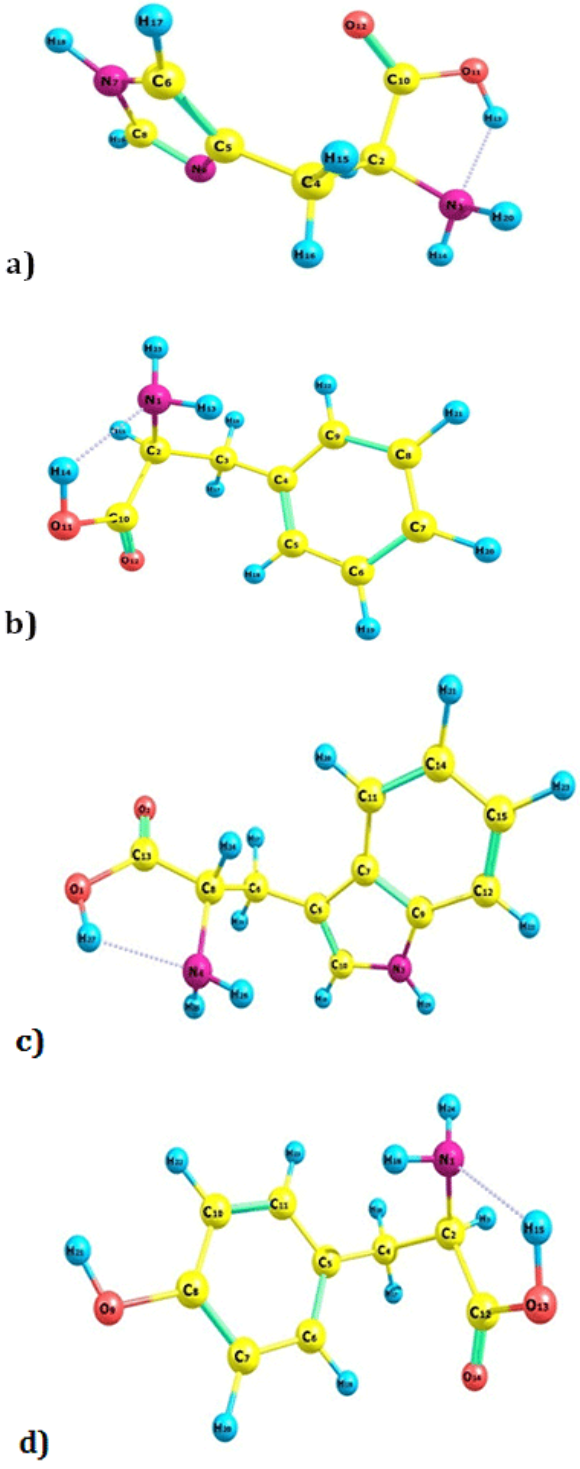


**Figure 1:** Graphical sketches of the optimized molecular structures of a) Histidine, b) Phenylalanine, c) Tryptophan and d) Tyrosine showing the numbering of the atoms.

The analysis of the results obtained in the study aimed at verifying that the KID procedure was fulfilled. On doing it previously, several descriptors associated with the results that the HOMO and LUMO calculations obtained are related with results obtained using the vertical I and A following the $\Delta SCF$ procedure. A link exists between the three main descriptors and the simplest conformity to the Koopmans' theorem by linking $\in_H$ with -I, $\in_L$ with -A, and their behavior in describing the HOMO-LUMO gap as $J_I = |\in_H + Egs(N-1) - Egs(N)|$, $J_I = |\in_L + Egs(N) - Egs(N+1)|$ and $J_{HL} = \sqrt{J_I^2 + J_A^2}$ 2. Notably, the $J_A$ descriptor consists of an approximation that remains valid only when the HOMO that a radical anion has (the SOMO) shares similarity with the LUMO of the neutral system. Consequently, we decided to design another descriptor $\Delta SL$, to guide in verifying the accuracy of the approximation [13-20]. The results of this analysis are presented in Table 1 to 4 for Histidine, Phenylalanine, Tryptophan and Tyrosine, respectively.

**Table 1:** Electronic energies of the neutral, positive and negative molecular systems (in au) of Histidine, the HOMO, LUMO and SOMO orbital energies (also in au), $J_I$, $J_A$, $J_{HL}$ and ΔSL descriptors calculated with the eight density functionals and the Def2TZVP basis set using water as solvent simulated with the SMD parameterization of the IEF-PCM model.

| | Eo | E+ | E- | HOMO | LUMO | SOMO | J(I) | J(A) | J(HL) | ΔSL |
|---|---|---|---|---|---|---|---|---|---|---|
| CAM-B3LYP | -548.81 | -548.59 | -548.84 | -0.277 | 0.033 | -0.094 | 0.059 | 0.063 | 0.086 | 0.126 |
| LC-ωPBE | -548.70 | -548.48 | -548.74 | -0.326 | 0.078 | -0.143 | 0.105 | 0.110 | 0.152 | 0.222 |
| M11 | -548.83 | -548.61 | -548.84 | -0.319 | 0.054 | -0.116 | 0.095 | 0.058 | 0.111 | 0.170 |
| MN12SX | -548.63 | -548.42 | -548.66 | -0.219 | -0.043 | -0.035 | 0.002 | 0.014 | 0.014 | 0.008 |
| N12SX | -548.81 | -548.60 | -548.84 | -0.215 | -0.023 | -0.032 | 0.002 | 0.005 | 0.005 | 0.008 |
| ωB97 | -548.96 | -548.75 | -548.99 | -0.321 | 0.083 | -0.136 | 0.105 | 0.108 | 0.151 | 0.219 |
| ωB97X | -548.91 | -548.70 | -548.28 | -0.313 | 0.074 | -0.103 | 0.096 | 0.563 | 0.572 | 0.178 |
| ωB97XD | -548.87 | -548.66 | -548.90 | -0.297 | 0.059 | -0.110 | 0.080 | 0.085 | 0.117 | 0.170 |

**Table 2:** Electronic energies of the neutral, positive and negative molecular systems (in au) of Phenylalanine, the HOMO, LUMO and SOMO orbital energies (also in au), $J_I$, $J_A$, $J_{HL}$ and ΔSL descriptors calculated with the eight density functionals and the Def2TZVP basis set using water as solvent simulated with the SMD parameterization of the IEF-PCM model.

| | Eo | E+ | E- | HOMO | LUMO | SOMO | J(I) | J(A) | J(HL) | ΔSL |
|---|---|---|---|---|---|---|---|---|---|---|
| CAM-B3LYP | -554.8 | -554.55 | -554.82 | -0.304 | 0.024 | -0.078 | 0.058 | 0.05 | 0.077 | 0.102 |
| LC-ωPBE | -554.69 | -554.44 | -554.73 | -0.353 | 0.062 | -0.135 | 0.102 | 0.097 | 0.141 | 0.196 |
| M11 | -554.81 | -554.56 | -554.84 | -0.345 | 0.05 | -0.105 | 0.093 | 0.074 | 0.119 | 0.155 |
| MN12SX | -554.63 | -554.39 | -554.67 | -0.249 | -0.042 | -0.041 | 0.002 | 0.005 | 0.005 | 0.001 |
| N12SX | -554.83 | -554.59 | -554.86 | -0.243 | -0.03 | -0.037 | 0.003 | 0.004 | 0.005 | 0.007 |
| ωB97 | -554.96 | -554.99 | -554.99 | -0.347 | 0.066 | -0.127 | 0.376 | 0.095 | 0.388 | 0.193 |
| ωB97X | -554.92 | -554.67 | -554.3 | -0.34 | 0.06 | -0.113 | 0.094 | 0.561 | 0.569 | 0.173 |
| ωB97XD | -554.88 | -554.91 | -554.91 | -0.324 | 0.048 | -0.109 | 0.353 | 0.077 | 0.362 | 0.157 |

**Table 3:** Electronic energies of the neutral, positive and negative molecular systems (in au) of Tryptophan, the HOMO, LUMO and SOMO orbital energies (also in au), $J_I$, $J_A$, $J_{HL}$ and ΔSL descriptors calculated with the eight density functionals and the Def2TZVP basis set using water as solvent simulated with the SMD parameterization of the IEF-PCM model.

| | Eo | E+ | E- | HOMO | LUMO | SOMO | J(I) | J(A) | J(HL) | ΔSL |
|---|---|---|---|---|---|---|---|---|---|---|
| CAM-B3LYP | -686.37 | -686.17 | -686.41 | -0.259 | 0.018 | -0.092 | 0.054 | 0.055 | 0.077 | 0.11 |
| LC-ωPBE | -686.24 | -686.03 | -686.28 | -0.305 | 0.052 | -0.136 | 0.095 | 0.093 | 0.133 | 0.188 |
| M11 | -686.39 | -686.18 | -686.43 | -0.299 | 0.043 | -0.125 | 0.086 | 0.083 | 0.119 | 0.168 |
| MN12SX | -686.18 | -685.97 | -686.21 | -0.206 | -0.044 | -0.042 | 0.002 | 0.005 | 0.006 | 0.002 |
| N12SX | -686.42 | -686.22 | -686.45 | -0.201 | -0.032 | -0.04 | 0.002 | 0.004 | 0.004 | 0.008 |
| ωB97 | -686.58 | -686.37 | -686.61 | -0.3 | 0.057 | -0.128 | 0.094 | 0.092 | 0.131 | 0.185 |
| ωB97X | -686.52 | -686.31 | -685.76 | -0.293 | 0.051 | -0.115 | 0.087 | 0.709 | 0.714 | 0.167 |
| ωB97XD | -686.48 | -686.27 | -686.51 | -0.279 | 0.041 | -0.112 | 0.075 | 0.076 | 0.107 | 0.153 |

**Table 4:** Electronic energies of the neutral, positive and negative molecular systems (in au) of Tyrosine, the HOMO, LUMO and SOMO orbital energies (also in au), $J_I$, $J_A$, $J_{HL}$ and ΔSL descriptors calculated with the eight density functionals and the Def2TZVP basis set using water as solvent simulated with the SMD parameterization of the IEF-PCM model.

| | Eo | E+ | E- | HOMO | LUMO | SOMO | J(I) | J(A) | J(HL) | ΔSL |
|---|---|---|---|---|---|---|---|---|---|---|
| CAM-B3LYP | -630.05 | -629.82 | -630.08 | -0.28 | 0.021 | -0.093 | 0.057 | 0.056 | 0.08 | 0.114 |
| LC-ωPBE | -629.92 | -629.69 | -629.96 | -0.327 | 0.059 | -0.138 | 0.1 | 0.097 | 0.139 | 0.197 |
| M11 | -630.07 | -629.84 | -630.1 | -0.321 | 0.048 | -0.127 | 0.091 | 0.085 | 0.124 | 0.174 |
| MN12SX | -629.85 | -629.63 | -629.89 | -0.226 | -0.042 | -0.043 | 0.002 | 0.003 | 0.003 | 0.001 |
| N12SX | -630.07 | -629.85 | -630.1 | -0.22 | -0.032 | -0.039 | 0.002 | 0.004 | 0.004 | 0.008 |
| ωB97 | -630.22 | -630 | -630.26 | -0.321 | 0.063 | -0.13 | 0.099 | 0.095 | 0.137 | 0.193 |
| ωB97X | -630.17 | -629.95 | -629.46 | -0.315 | 0.057 | -0.117 | 0.092 | 0.656 | 0.663 | 0.174 |
| ωB97XD | -630.13 | -629.91 | -630.16 | -0.3 | 0.046 | -0.112 | 0.078 | 0.078 | 0.11 | 0.158 |

As Tables 1 to 4 provide, the KID procedure applies accurately for the MN12SX and N12SX density functionals that are range-separated hybrid meta-NGA as well as range-separated hybrid NGA density functionals respectively. In fact, the values of $J_I$, $J_A$ and $J_{HL}$ are actually not zero. Nevertheless, the results tend to be impressive especially for the MN12SX density functional. As well, the $\Delta SL$ descriptor reaches the minimum values when MN12SX and N12SX density functionals are used in the calculations. This implies that there are sufficient justifications to assume that the LUMO of the neutral approximates the electron affinity.

## Calculation of the Maximum Absorption Wavelength

Being aromatic amino acids, the molecules considered here will absorb energy in the UV region of the electromagnetic spectrum and they would be best studied using the Time-Dependent Density Functional Theory (TDDFT). In the past, various TDDFT studies of molecules of different size have used optimally-tuned RSH density functionals [29, 30, 32, 33, 35, 49-63]. The considerable success of the approach is however undermined by the issue of tuning being system dependent. Therefore, focus should be on establishing the effectiveness of the behaviors of the fixed RSH density functionals in describing the excitation characteristics. In his works, Becke has recently mentioned that the adiabatic connection and the ideas of Hohenberg, Kohn, and Sham apply only to electronic ground states is a common misconception [64]. Furthermore, consistent with Baerends et al., KS model is not appreciated for being superior because of its lowest excitation energy in molecules. Physically, it amounts to an excitation of the KS system rather than electron addition as would be the case in Hartree-Fock. Thus, it can be effectively be used as a measure of the optical gap and is an effective approximation to the gap (in molecules) [65]. In their conclusion, van Meer et al. advanced that the HOMO-LUMO gap associated with the KS model tends to be an approximation of the lowest excitation energy, a desirable characteristic with no concerns regarding it [66] (Figure 2).

Therefore, the calculation of the maximum wavelength absorption of these amino acids involved conducting ground state calculations with the aforementioned eight density functionals at the same level of model chemistry and theory and determining the HOMO-LUMO gap. Figure 1 provides an illustration that

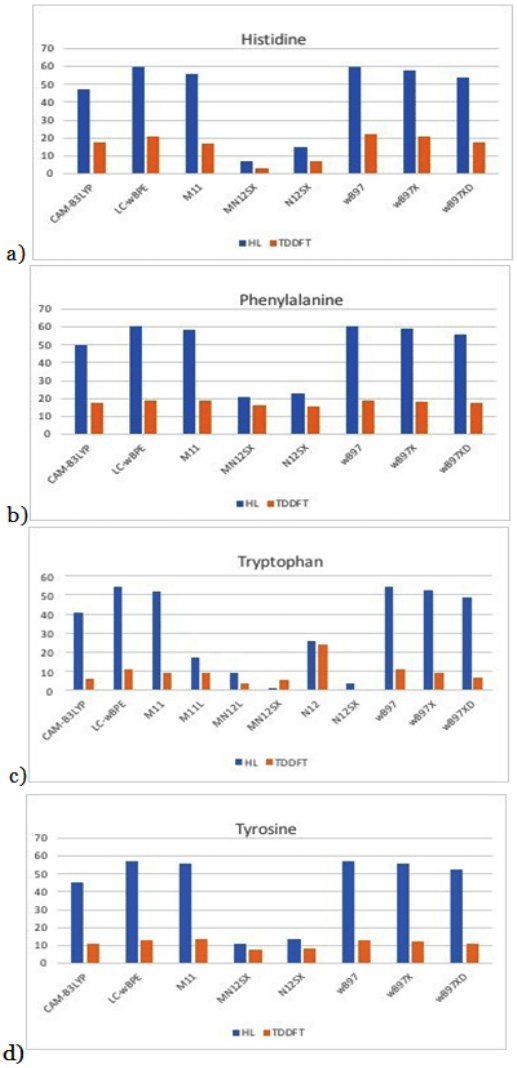


**Figure 2:** Graphical sketches of the differences between the calculated maximum absorption wavelengths and experimental values (in nm) of a) Histidine, b) Phenylalanine, c) Tryptophan and d) Tyrosine by direct comparison with the value of the HOMO-LUMO gap (HL) or through a TDDFT calculation (TDDFT).

compares graphically the results involved in the ground-state approximation derived from the HOMO-LUMO gap together with the TDDFT results with the known experimental values for the molecules (Histidine = 211 nm, Phenylalanine = 257.5 nm, Tryptophan = 278 nm and Tyrosine = 274.25 nm) [67].

Notably, the presented results suggest that the differences with the experimental value for $\lambda_{max}$ tend to have the same order in the various functionals that the current study considers. If the $\lambda_{max}$ values that the HOMO-LUMO gap generates were the ones considered, MN12SX and N12SX would appear to be specially accurate in predicting this value. Such finding does not apply in the rest of the density functionals that this study considered.

## Global Descriptors Calculation

As can be seen from Tables 1 to 4, the results for the descriptors show values that are consistent with our previous findings for the case of the melanoidins and peptides of marine origin, that is, the MN12SX density functional is capable of giving HOMO and LUMO energies that allow to verify the agreement with the approximate Koopmans' theorem [13-20]. This is not only true because the $J_{HL}$ values are almost, zero, but due to the fact that the ΔSL descriptor, which relates to the difference between the LUMO of the neutral and the HOMO of the anion, is also close to zero. Indeed, these values cannot be exactly equal to zero, but the small differences mean that errors in the prediction of the global reactivity descriptors will be negligible. Moreover, it can be seen from Tables 1 to 4 that the MN12SX density functional predict negative values for the LUMO energies which will represent positive values of the electron affinity A.

The KID procedure has its foundations on the behavior of the four descriptors $J_I, J_A, J_{HL}$ , and $\Delta SL$ : the closer they are to zero the better agreement of a density functional in giving accurate CDFT descriptors calculated only from the HOMO and LUMO. This allows to avoid the calculation of the energies of the cation and anion species which being open systems are more difficult to converge than the parent neutral molecule, that is inconvenient when studying large systems like those considered in this study.

By taking into account the KID procedure presented in our previous works together with the finite difference approximation, the global reactivity descriptors can be expressed as:

Electronegativity $\chi = -\frac{1}{2}(I + A) \approx \frac{1}{2}(\in_L + \in_H)$ [5,6]

Global Hardness $\eta = (I - A) \approx (\in_L - \in_H)$ [5, 6]

Electrophilicity $\omega = \frac{\mu^2}{2\eta} = \frac{(I + A)^2}{4(I - A)} \approx \frac{(\in_L + \in_H)^2}{4(\in_L - \in_H)}$ [68]

Electrodonating Power $\omega^- = \frac{(3I + A)^2}{16(I - A)} \approx \frac{(3 \in_H + \in_L)^2}{16\eta}$ [69]

Electroaccepting Power $\omega^+ = \frac{(I + 3A)^2}{16(I - A)} \approx \frac{(\in_H + 3 \in_L)^2}{16\eta}$ [69]

Net Electrophilicity $\Delta\omega^{\pm} = \omega^+ - (-\omega^-) = \omega^+ + \omega^-$ [70]

where $\in_H$ and $\in_L$ are the energies of the HOMO and LUMO, respectively. According to our previous discussion, the results for the global reactivity descriptors based on the values of the HOMO and LUMO energies calculated with the MN12SX density functional are presented in Table 5 which illustrates the results obtained after calculating for the electronegativity $\chi$, chemical hardness $\eta$, global electrophilicity $\omega$, electroaccepting ($\omega+$) and electrodonating ($\omega-$) powers as well as net electrophilicity with the MN12SX density. The Def2TZVP basis set is used with water acting as a solvent in line with the SMD solvation model.

**Table 5:** Global reactivity descriptors for the four standard aromatic amino acids calculated with the MN12SX density functional.

| | **Electronegativity (χ)** | **Chemical Hardness (η)** | **Electrophilicity (ω)** |
|---|---|---|---|
| Histidine | 3.5551 | 4.7941 | 1.3182 |
| Phenylalanine | 3.9521 | 5.6202 | 1.3896 |
| Tryptophan | 3.398 | 4.4069 | 1.31 |
| Tyrosine | 3.6407 | 5.0186 | 1.3206 |
| | **Electrodonating Power (ω−)** | **Electroaccepting Power (ω+)** | **Net Electrophilicity (Δω±)** |
| Histidine | 2.7716 | 1.374 | 4.1457 |
| Phenylalanine | 3.0027 | 1.4276 | 4.4303 |
| Tryptophan | 2.7016 | 1.3787 | 4.0803 |
| Tyrosine | 2.8079 | 1.3686 | 4.1764 |

## Quantification of the AGEs Inhibitor Ability

The Maillard reaction between a reducing carbonyl and the amino group of a peptide or protein leads to the formation of a Schiff base which through a series of steps renders different molecules known as Advanced Glycation Endproducts or AGEs. It is believed that the presence of these AGEs is one of the main reasons for the developing of some diseases like Diabetes, Alzheimer and Parkinson [71].

Among several strategies that have been considered for the prevention of the formation of AGEs, it is worth to mention the use of compounds presenting amino groups in their

structure capable of interacting with the reducing carbonyl of carbohydrates and being competitive with the amino acids, pep- tides and proteins present in our body. Many compounds have been devised as drugs to achieve this goal and to name a few; we can include Pyridoxamine, Aminoguanidine, Carnosine, Metformin, Pioglitazone and Tenilsetam [72, 73].

It can be proposed that peptides having amino and amido groups could be thought as potential therapeutic drugs for preventing the formation of AGEs because they could in the Maillard reaction with reducing carbohydrates before than the peptides and proteins of our body. Although this a merely speculative proposal, we believe that it is worth to explore this possibility by following a methodology earlier presented by us. In a previous work, we have studied the ability of a group of proposed molecules to act as inhibitors of the formation of AGEs by quantifying their behavior in terms of CDFT reactivity descriptors [10]. It was concluded that the key factor in the study of the chemical reactivity of the potential AGEs inhibitors was on their nucleophilic character and although there are several definitions of nucleophilicity, our results suggested that the inverse of the net electrophilicity could be a good definition for the nucleophilicity N [74]. On the basis of the mentioned analysis, we were able to find some qualitative trends for the studied molecular systems.

In this work, we will extend this correlation to the four standard aromatic amino acids in order to see if they can be considered as precursors of therapeutic drugs as nutraceuticals for the inhibition of the formation of AGEs. As the model chemistry employed in both works is the same, the comparison is straightforward:

Aminoguanidine > Metformin > Tryptophan > Histidine > Tyrosine > Phenylalanine > Carnosine > Tenilsetam > Pyridoxamine > Pioglitazone

This qualitative trend is representative of the known pharmacological properties of the studied AGEs inhibitors [72, 73] and it can be seen that the studied amino acids possess AGEs Inhibitor abilities similar to that of Metformin or Carnosine if we rely only in the mentioned criteria. However, the AGEs inhibition ability could also depend on many other factors. Thus, additional information will be needed to fully support this conclusion.

## Bioactivity Scores

When considering a given molecular system as a potential therapeutic drug, it is customary to check if the considered species follows the Lipinsky Rule of Five which is used to predict whether a compound has or not has a drug-like character [75]. The molecular properties related to the drug-like character were calculated with the aid of the MolSoft and Molinspiration software and are presented in Table 6 where miLogP represents the octanol/water partition coefficient, TPSA is the molecular polar surface area, n atoms is the number of atom of the molecule, nON and nOHNH are the number of hydrogen bond acceptors and hydrogen bond donors respectively, nviol is the number of violations of the Lipinsky Rule of Five, nrotb is the number of rotatable bonds, volume is the molecular volume, and MW is the molecular weight of the studied system.

**Table 6**: Molecular properties of the four standard aromatic amino acids calculated to verify the Lipinsky Rule of Five.

| Molecule | miLogP | TPSA | nAtoms | nON | nOHNH | nviol | nrotb | volume | MW |
|---|---|---|---|---|---|---|---|---|---|
| Histidine | -3.00 | 92.00 | 11 | 5 | 4 | 0 | 3 | 136.79 | 155.16 |
| Phenylalanine | -1.23 | 63.32 | 12 | 3 | 3 | 0 | 3 | 155.96 | 165.19 |
| Tryptophan | -1.08 | 79.11 | 15 | 4 | 4 | 0 | 3 | 184.94 | 204.23 |
| Tyrosine | -1.71 | 83.55 | 13 | 4 | 4 | 0 | 3 | 163.98 | 181.19 |

However, what the Lipinsky Rule of Five really measures is the oral bioavailability of a potential drug because this is desired property for a molecule having drug-like character. Indeed, this criteria cannot be applied to peptides, even when they are small, as we can see from Table 1-6, due to the inherent molecular weight and number of hydrogen bonds.

In a more recent work, Martin have developed what she called "A Bioavailability Score" (ABS) for avoiding these problems [76]. The rule for the ABS established that the Bioavailability Score for neutral organic molecules must be 0.55 if they pass the Lipinsky Rule of Five and 0.170 if they fail. The ABS value for all the amino acids considered in this work have been calculated by using the ChemDoodle software and the results were equal to 0.170 for all of them.

Then, a different approach was followed by considering similarity searches in the chemical space of compounds with structures that can be compared to those that are being studied and with known pharmacological properties. As has been mentioned in the Settings and Computational Methods section, this task can be accomplished using the online Molinspiration software for the prediction of the bioactivity score for different drug targets (GPCR ligands, kinase inhibitors, ion channel modulators, enzymes and nuclear receptors). The results are named Bioactivity Scores and the values for the standard aromatic amino acids are presented in Table 7.

**Table 7**: Bioactivity scores of the standard aromatic amino acids calculated on the basis of GPCR Ligand, Ion Channel Modulator, Nuclear Receptor Ligand, Kinase Inhibitor, Protease Inhibitor and Enzyme Inhibitor interactions.

| Molecule | GPCR Ligand | Ion Channel Modulator | Kinase Inhibitor | Nuclear Receptor Ligand | Protease Inhibitor | Enzyme Inhibitor |
|---|---|---|---|---|---|---|
| Histidine | 0.36 | 0.77 | –0.45 | -1.84 | 0.33 | 0.84 |
| Phenylalanine | –0.22 | 0.34 | -0.89 | -0.53 | -0.09 | 0.16 |
| Tryptophan | 0.33 | 0.54 | -0.13 | -0.22 | 0.15 | 0.44 |
| Tyrosine | -0.08 | 0.41 | -0.68 | -0.20 | -0.04 | 0.27 |

These bioactivity scores for organic molecules can be interpreted as active (when the bioactivity score > 0), moderately active (when the bioactivity score lies between -5.0 and 0.0) and inactive (when the bioactivity score < -5.0). All the Mirabamides A-H were found to be moderately bioactive towards all the enzymes considered for the study.

## Conclusions

This study assessed eight density functionals that include CAM-B3LYP, LC-ωPBE, M11, MN12SX, N12SX, ωB97, ωB97X and ωB97XD related to the Def2TZVP basis sets together with the SMD solvation model in the calculation of the molecular properties and structures of the four standard aromatic amino acids: Histidine, Phenylalanine, Tryptophan and Tyrosine.

The global chemical reactivity descriptors for the systems were calculated via the Conceptual Density Functional Theory (CDFT). The prediction of the maximum absorption wavelength directly from the HOMO-LUMO tends to be considerably accurate relative to the experimental values for the MN12SX density functional.

Otherwise, the ability of the studied molecules in acting as efficient inhibitors of the formation of Advanced Glycation Endproducts (AGEs) (perhaps as nutraceuticals), which constitutes a useful knowledge for the development of drugs for fighting Diabetes, Alzheimer and Parkinson diseases.

Finally, the bioactivity scores for the four standard aromatic amino acids are predicted through different methodologies.

## Acknowledgements

This work has been partially supported by CIMAV, SC and Consejo Nacional de Ciencia y Tecnologia (CONACYT, Mexico) through Grant 219566- 2014 for Basic Science Research. Daniel Glossman-Mitnik conducted this work while a Visiting Lecturer at the University of the Balearic Islands from which support is gratefully acknowledged. Norma Flores-Holguin and Daniel Glossman-Mitnik are researchers of CIMAV and CONACYT. This work was cofunded by the Ministerio de Economia y Competitividad (MINECO) and the European Fund for Regional Development (FEDER) (CTQ2014-55835-R

## References

1. La Barre S and Kornprobst JM. Outstanding Marine Molecules. Wiley-Blackwell, Weinheim, 2014.
2. Kim S K. Marine Proteins and Peptides - Biological Activities and Applications. Wiley-Blackwell, Chichester, UK, 2013.
3. Rekka E and Kourounakis P. Chemistry and Molecular Aspects of Drug Design and Action. CRC Press, Boca Raton, 2008.
4. N´aray-Szab´o G and Warshel A. Computational Approaches to Biochemical Reactivity. Kluwer Academic Publishers, New York, 2002.
5. Parr R, Yang W. Density-Functional Theory of Atoms and Molecules. Oxford University Press, New York, 1989.
6. Geerlings P, De Proft F, Langenaeker W. Conceptual Density Functional Theory. Chem Rev. 2003;103(5):1793-1873.
7. Ayers P, Parr R. The Variational Principles for Describing Chemical Reactions: The Fukui Function and Chemical Hardness Revisited. J Am Chem Soc. 2000;122(9):2010-2018.
8. Poater A, Saliner AG, Carbó-Dorca R, Poater J, Solà M, Cavallo L, et al. Modeling the Structure-Property Relationships of Nanoneedles: A Journey Toward Nanomedicine. J Comput Chem. 2009;30(2):275-284. doi: 10.1002/jcc.21041
9. Poater A, Gallegos Saliner A, Solà M, Cavallo L, Worth AP. Computational methods to predict the reactivity of nanoparticles through structure-property relationships. Expert Opin Drug Deliv. 2010;7(3):295-305. doi: 10.1517/17425240903508756
10. Frau J, Glossman-Mitnik D. Chemical Reactivity Theory Study of Advanced Glycation Endproduct Inhibitors. Molecules. 2017;22(1):226.
11. Gupta GK and Kumar V. Chemical Drug Design. Walter de Gruyter GmbH, Berlin, 2016.
12. Gore M and Jagtap UB, Computational Drug Discovery and Design. Springer Science+Business Media, LLC, New York, 2018.
13. Frau J, Glossman-Mitnik D. Molecular Reactivity and Absorption Properties of Melanoidin Blue-G1 through Conceptual DFT. Molecules. 2018;23(3):E559. doi: 10.3390/molecules23030559
14. Frau J, Glossman-Mitnik D. Conceptual DFT Study of the Local Chemical Reactivity of the Dilysyldipyrrolones A and B Intermediate Melanoidins. Theoretical Chemistry Accounts. 2018;137(5):67.
15. Frau J, Glossman-Mitnik D. Conceptual DFT Study of the Local Chemical Reactivity of the Colored BISARG Melanoidin and Its Protonated Derivative. Front Chem. 2018;6(136):1-9. doi: 10.3389/fchem.2018.00136

16. Frau J, Glossman-Mitnik D. Molecular Reactivity of some Maillard Reaction Products Studied through Conceptual DFT. Contemporary Chemistry. 2018;1(1):1-14.
17. Frau J, Glossman-Mitnik D. Computational Study of the Chemical Reactivity of the Blue-M1 Intermediate Melanoidin. Computational and Theoretical Chemistry. 2018;1134:22-29.
18. Frau J, Glossman-Mitnik D. Chemical Reactivity Theory Applied to the Calculation of the Local Reactivity Descriptors of a Colored Maillard Reaction Product. Chemical Science International Journal. 2018;22(4):1-14.
19. Frau J, Glossman-Mitnik D. Blue M2: An Intermediate Melanoidin Studied via Conceptual DFT. J Mol Model. 2018;24(6):138. doi: 10.1007/s00894-018-3673-0
20. Frau J, Flores-Holguin N, Glossman-Mitnik D. Chemical Reactivity Properties, pKa Values, AGEs Inhibitor Abilities and Bioactivity Scores of the Mirabamides A–H Peptides of Marine Origin Studied by Means of Conceptual DFT. Mar Drugs. 2018;16(9):302-319. doi: 10.3390/md16090302
21. Lewars E. Computational Chemistry - Introduction to the Theory and Applications of Molecular and Quantum Mechanics. Kluwer Academic Publishers, Dordrecht, 2003.
22. Young D. Computational Chemistry - A Practical Guide for Applying Techniques to Real-World Problems. John Wiley & Sons, New York, 2001.
23. Jensen F. Introduction to Computational Chemistry. 2nd Edition, John Wiley & Sons, Chichester, England, 2007.
24. Cramer. Essentials of Computational Chemistry - Theories and Models, 2nd Edition, John Wiley & Sons, Chichester, England, 2004.
25. Iikura H, Tsuneda T, Yanai T, Hirao K. A Long-Range Correction Scheme for Generalized-Gradient-Approximation Exchange Functionals. The Journal of Chemical Physics. 2001;115(8):3540-3544.
26. Chai JD, Head-Gordon M. Long-Range Corrected Hybrid Density Functionals with Damped Atom-Atom Dispersion Corrections. Physical Chemistry Chemical Physics. 2008;10:6615-6620.
27. Yanai T, Tew DP, Handy NC. A New Hybrid Exchange-Correlation Functional Using the Coulomb-Attenuating Method (CAM-B3LYP). Chemical Physics Letters. 2004;393(1-3):51-57.
28. Heyd J, Scuseria GE. Efficient Hybrid Density Functional Calculations in Solids: Assessment of the Heyd-Scuseria-Ernzerhof Screened Coulomb Hybrid Functional. J Chem Phys. 2004;121(3):1187-1192. doi: 10.1063/1.1760074
29. Stein T, Kronik L, Baer R. Reliable Prediction of Charge Transfer Excitations in Molecular Complexes Using Time-Dependent Density Functional Theory. J Am Chem Soc. 2009;131(8):2818-2820. doi: 10.1021/ja8087482
30. Stein T, Kronik L, Baer R. Prediction of Charge-Transfer Excitations in Coumarin-Based Dyes Using a Range-Separated Functional Tuned From First Principles. J Chem Phys. 2009;131(24):244119. doi: 10.1063/1.3269029
31. Stein T, Eisenberg H, Kronik L, Baer R. Fundamental Gaps in Finite Systems from Eigenvalues of a Generalized Kohn-Sham Method. Phys Rev Lett. 2010;105(26):266802-266804. doi: 10.1103/PhysRevLett.105.266802
32. Karolewski A, Stein T, Baer R, Kummel S. Communication: Tailoring the Optical Gap in Light-Harvesting Molecules. J Chem Phys. 2011;134(15):151101-151105. doi: 10.1063/1.3581788
33. Kuritz N, Stein T, Baer R, Kronik L. Charge-Transfer-Like $\pi \rightarrow \pi^*$ Excitations in Time-Dependent Density Functional Theory: A Conundrum and Its Solution. J Chem Theory Comput. 2011;7(8):2408-2415. doi: 10.1021/ct2002804
34. Ansbacher T, Srivastava HK, Stein T, Baer R, Merkx M, Shurki A. Calculation of Transition Dipole Moment in Fluorescent Proteins-Towards Efficient Energy Transfer. Phys Chem Chem Phys. 2012;14(12):4109-4117. doi: 10.1039/c2cp23351g
35. Kronik L, Stein T, Refaely-Abramson S, Baer R. Excitation Gaps of Finite-Sized Systems from Optimally Tuned Range-Separated Hybrid Functionals. J Chem Theory Comput. 2012;8(5):1515-1531. doi: 10.1021/ct2009363
36. Stein T, Autschbach J, Govind N, Kronik L, Baer R. Curvature and Frontier Orbital Energies in Density Functional Theory. Journal of Physical Chemistry Letters. 2012;3(24):3740-3744. doi: 10.1021/jz3015937
37. Halgren TA. Merck Molecular Force Field. I. Basis, Form, Scope, Parameterization, and Performance of MMFF94. Journal of Computational Chemistry. 1996;17(5-6):490-519.
38. Halgren TA. Merck Molecular Force Field. II. MMFF94 van der Waals and Electrostatic Parameters for Intermolecular Interactions. Journal of Computational Chemistry. 1996;17(5-6):520-552.
39. Halgren TA. MMFF VI. MMFF94s Option for Energy Minimization Studies. Journal of Computational Chemistry. 1999;20(7):720-729.
40. Halgren TA, Nachbar RB. Merck Molecular Force Field. IV. Conformational Energies and Geometries for MMFF94. Journal of Computational Chemistry. 1996;17(5-6):587-615.
41. Halgren TA. Merck Molecular Force field. V. Extension of MMFF94 Using Experimental Data, Additional Computational Data, and Empirical Rules. Journal of Computational Chemistry. 1996;17(5-6):616-641.
42. Frisch MJ, Trucks GW, Schlegel HB, Scuseria GE, Robb MA and Cheeseman R et al. Gaussian 09 Revision E.01, Gaussian Inc., Wallingford CT, 2016.
43. Weigend F, Ahlrichs R. Balanced Basis Sets of Split Valence, Triple Zeta Valence and Quadruple Zeta Valence Quality for H to Rn: Design and Assessment of Accuracy. Phys Chem Chem Phys. 2005;7(18):3297-3305. doi: 10.1039/b508541a
44. Weigend F. Accurate Coulomb-fitting Basis Sets for H to Rn. Phys Chem Chem Phys. 2006;8(9):1057-1065. doi: 10.1039/b515623h
45. Marenich AV, Cramer CJ, Truhlar DG. Universal Solvation Model Based on Solute Electron Density and a Continuum Model of the Solvent Defined by the Bulk Dielectric Constant and Atomic Surface Tensions. J Phys Chem B.1 2009;113(18):6378-6396. doi: 10.1021/jp810292n
46. Henderson TM, Izmaylov AF, Scalmani G, Scuseria GE. Can Short-Range Hybrids Describe Long-Range-Dependent Properties? J Chem Phys. 2009;131(4):044108. doi: 10.1063/1.3185673
47. Peverati R, Truhlar DG. Improving the Accuracy of Hybrid Meta-GGA Density Functionals by Range Separation. The Journal of Physical Chemistry Letters. 2011;2(21):2810-2817.

48. Peverati R, Truhlar DG. Screened-Exchange Density Functionals with Broad Accuracy for Chemistry and Solid-State Physics. Physical Chemistry Chemical Physics. 2012;14(47):16187-16191.
49. Egger DA, Weissman S, Refaely-Abramson S, Sharifzadeh S, Dauth M, Baer R, et al. Outer-Valence Electron Spectra of Prototypical Aromatic Heterocycles From an Optimally Tuned Range-Separated Hybrid Functional. J Chem Theory Comput. 2014;10(5):1934-1952. doi: 10.1021/ct400956h
50. Foster ME, Wong BM. Nonempirically Tuned Range-Separated DFT Accurately Predicts Both Fundamental and Excitation Gaps in DNA and RNA Nucleobases. Journal of Chemical Theory and Computation. 2012;8(8):2682-2687.
51. Foster ME, Azoulay JD, Wong BM, Allendorf MD. Novel Metal–Organic Framework Linkers for Light Harvesting Applications. Chemical Science. 2014;5(5):2081-2090.
52. Jacquemin D, Moore B, Planchat A, Adamo C, Autschbach J. Performance of an Optimally Tuned Range-Separated Hybrid Functional for 0-0 Electronic Excitation Energies. J Chem Theory Comput. 2014;10(4):1677-1685. doi: 10.1021/ct5000617
53. Karolewski A, Kronik L, Kummel S. Using Optimally Tuned Range Separated Hybrid Functionals in Ground-State Calculations: Consequences and Caveats. J Chem Phys. 2013;138(20):204115. doi: 10.1063/1.4807325
54. Koppen JV, Hapka M, Szczeniak MM, Chalasinski G. Optical Absorption Spectra of Gold Clusters Au(n) (n = 4, 6, 8,12, 20) From Long-Range Corrected Functionals with Optimal Tuning. J Chem Phys. 2012;137(11):114302.
55. Lima IT, Prado Ada S, Martins JB, de Oliveira Neto PH, Ceschin AM, da Cunha WF, et al. Improving the Description of the Optical Properties of Carotenoids by Tuning the Long-Range Corrected Functionals. J Phys Chem A. 2016;120(27):4944-4950. doi: 10.1021/acs.jpca.5b12570
56. Manna AK, Lee MH, McMahon KL, Dunietz BD. Calculating High Energy Charge Transfer States Using Optimally Tuned Range- Separated Hybrid Functionals. J Chem Theory Comput. 2015;11(3):1110-1117. doi: 10.1021/ct501018n
57. Li BM, Autschbach J. Longest-Wavelength Electronic Excitations of Linear Cyanines: The Role of Electron Delocalization and of Approximations in Time-Dependent Density Functional Theory. J Chem Theory Comput. 2013;9(11):4991-5003. doi: 10.1021/ct400649r
58. Niskanen M, Hukka TI. Modeling of Photoactive Conjugated Donor-Acceptor Copolymers: the Effect of the Exact HF Exchange in DFT Functionals on Geometries and Gap Energies of Oligomer and Periodic Models. Phys Chem Chem Phys. 2014;16(26):13294-13305.
59. Pereira TL, Leal LA, da Cunha WF, Timoteo de Sousa Junior R, Ribeiro Junior LA, Antonio da Silva Filho D. Optimally Tuned Functionals Improving the Description of Optical and Electronic Properties of the Phthalocyanine Molecule. J Mol Model. 2017;23(3):71. doi: 10.1007/s00894-017-3246-7
60. Phillips H, Zheng S, Hyla A, Laine R, Geva E, Dunietz BD, et al. Ab Initio Calculation of the Electronic Absorption of Functionalized Octahedral Silsesquioxanes via Time-Dependent Density Functional Theory with Range-Separated Hybrid Functionals. J Phys Chem A. 2012;116(4):1137-1145. doi: 10.1021/jp208316t
61. Phillips H, Geva E, Dunietz BD. Calculating Off-Site Excitations in Symmetric Donor-Acceptor Systems via Time-Dependent Density Functional Theory with Range-Separated Density Functionals. J Chem Theory Comput. 2012;8(8):2661-2668. doi: 10.1021/ct300318g
62. Refaely-Abramson S, Baer R, Kronik L. Fundamental and Excitation Gaps in Molecules of Relevance for Organic Photovoltaics from an Optimally Tuned Range-Separated Hybrid Functional. Physical Review B. 2011;84(7):075144-075148.
63. Sun H, Autschbach J. Electronic Energy Gaps for π-Conjugated Oligomers and Polymers Calculated with Density Functional Theory. J Chem Theory Comput. 2014;10(3):1035-1047. doi: 10.1021/ct4009975
64. Becke AD. Vertical Excitation Energies from the Adiabatic Connection. J Chem Phys. 2016;145(19):194107. doi: 10.1063/1.4967813
65. Baerends EJ, Gritsenko OV, van Meer R. The Kohn-Sham Gap, the Fundamental Gap and the Optical Gap: The Physical Meaning of Occupied and Virtual Kohn-Sham Orbital Energies. Phys Chem Chem Phys. 2013;15(39):16408-16425. doi: 10.1039/c3cp52547c
66. Van Meer R, Gritsenko OV, Baerends EJ. Physical Meaning of Virtual Kohn-Sham Orbital's and Orbital Energies: An Ideal Basis for the Description of Molecular Excitations. J Chem Theory Comput. 2014;10(10):4432–4441. doi: 10.1021/ct500727c
67. Taniguchi M, Lindsey JS. Database of Absorption and Fluorescence Spectra of >300 Common Compounds for use in PhotochemCAD. Photochem Photobiol. 2018;94(2):290-327. doi: 10.1111/php.12860
68. Parr RG, Szentpaly LV, Liu S. Electrophilicity Index. Journal of the American Chemical Society. 1999;121(9):1922-1924.
69. Gazquez JL, Cedillo A, Vela A. Electrodonating and Electroaccepting Powers. J Phys Chem A. 2007;111(10):1966-1970. doi: 10.1021/jp065459f
70. Chattaraj PK, Chakraborty A, Giri S. Net Electrophilicity. J Phys Chem A. 2009;113(37):10068-10074. doi: 10.1021/jp904674x
71. Ahmed N. Advanced Glycation Endproducts - Role in Pathology of diabetic Complications. Diabetes Res Clin Pract. 2005;67(1):3-21. doi: 10.1016/j.diabres.2004.09.004
72. Rahbar S, Figarola JL. Novel Inhibitors of Advanced Glycation Endproducts. Arch Biochem Biophys. 2003;419(1):63-79.
73. Peyroux J, Sternberg M. Advanced glycation end products (AGEs): Pharmacological Inhibition in diabetes. Pathol Biol (Paris). 2006;54(7):405-419. doi: 10.1016/j.patbio.2006.07.006
74. Domingo LR, Perez P. The Nucleophilicity N index in Organic Chemistry. Org Biomol Chem. 2011;9(20):7168-7175. doi: 10.1039/c1ob05856h
75. Leeson P. Drug Discovery: Chemical Beauty Contest. Nature. 2012;481(7382):455-456.
76. Martin YC. A Bioavailability Score. Journal of Medicinal Chemistry. 2005;48(9):3164-3170.